AIAA JOURNAL
Vol. 32, No. 6, June 1994

Sound Radiation and Caustic Formation from a Point Source in a Wall Shear Layer

I. David Abrahams*
Keele University, Keele, Staffordshire ST5 5BG, England, United Kingdom
Gregory A. Kriegsmann†
New Jersey Institute of Technology, Newark, New Jersey 07102
and
Edward L. Reiss‡
Northwestern University, Evanston, Illinois 60208

The propagation of acoustic waves from a high-frequency point source in a shear layer flowing over an infinite rigid plate is considered. Asymptotic expansions of the solution are obtained as $k = \omega D/c_0 \to \infty$, using a previously developed method. Here, ω is the circular frequency of the point source, D is the thickness of the shear layer, and c_0 is the ambient sound speed. Stationary and moving sources are analyzed. An infinite sequence of caustic surfaces are created downstream of the source and adjacent to the wall, by the refraction of rays from the source and their subsequent reflection from the wall. The acoustic fields on and off the caustics are obtained. The vorticity of the acoustic field is large on a caustic, but it decays rapidly away from the "center" of the caustic surface. That is, the energy of the acoustic field on a caustic is localized. In addition, the caustic surfaces are "swept back" by the moving source. The striking similarity between the moving caustic surfaces and the experimentally determined coherent fluid structures, which originate in the laminar sublayer of a turbulent boundary layer and are localized regions of intense vorticity, suggests that the previously proposed mechanism for the formation of these localized coherent fluid structures might be valid. The bursting of these structures and the violent ejection of the fluid away from the sublayer could be one of the mechanisms producing turbulence in the boundary layer.

I. Introduction

WHEN a submerged vehicle (such as an airplane or a submarine) travels through a fluid, a boundary layer, which is in general turbulent, forms along the surface of the vehicle. Since the fluid must "stick" to this surface, there is a narrow region adjacent to the surface, which is called the laminar sublayer, in which the flow is laminar and strongly sheared.

Experimental results (e.g., Bushnell et al.,[1] Cantwell,[2] and Offen and Kline,[3] and references given therein) suggest that coherent fluid structures, which originate in the sublayer, burst and violently eject fluid up into the turbulent region of the boundary layer. Furthermore, it is believed that this bursting produces most of the turbulence and most of the noise generated in the turbulent boundary layer. These experiments further suggest that the coherent structures are localized regions of intense vorticity that propagate streamwise in the sublayer. Because of their vorticity, these structures gradually lift as they propagate downstream where they suddenly burst and eject their fluid upward. The precise mechanism for the formation of these structures has not been clearly ascertained, although several concepts have been proposed [e.g., hairpin vortex interactions (Falco[4])].

Since the bursting process is violent, it generates a relatively broad frequency spectrum of noise, as experimental results confirm. Thus, the bursting process produces waves that propagate through the boundary layer, in addition to other effects on the flow. The viscous drag and noise produced by the turbulent boundary layer are intimately related to the formation, propagation, and eventual bursting of these coherent structures. Any method for substantially reducing or controlling the bursting process will have a significant impact on vehicle drag reduction and noise suppression. Related large coherent flow structures also occur in other shear flows; e.g., for laminar boundary-layer flow at constant pressure they are called turbulent spots.

Structural vibrations and other turbulent boundary-layer fluctuations are additional noise sources that propagate waves in the boundary layer. These sources may also propagate waves through the structure of the vehicle which may then be emitted into the boundary layer. The wave field near the vehicle due to the noise propagation may be large and thus may dominate the reception of weak, scattered, or radiated fields from distant targets. If the precise nature of the noise field is known, then it may be possible to filter it from the total received signal to determine the desired distant signal. Furthermore, the noise produced by these sources and their interaction with the vehicle are radiated into the fluid. Knowledge of these noise mechanisms and their radiation patterns are essential for detection and surveillance and for the development of noise suppression techniques.

As an initial step toward analyzing these noise fields, we considered (Kriegsmann and Reiss[5]) the propagation of waves from a time-harmonic, monopole, uniform line source in a shear layer flowing above a rigid surface. We assumed that the shear flow does not vary in the spanwise direction, and hence we considered a two-dimensional problem. The resulting system of wave equations that are of third order correspond to an anisotropic, inhomogeneous, moving medium. Since the characteristic depth of the shear layer is often much greater than the acoustic wavelength of the source, the method of geometrical acoustics is used to obtain asymptotic approximations to the solution. For the bursting process this is equivalent to considering the high-frequency components of the burst; as a quantitative example, a fully developed turbulent boundary layer near the trailing edge of a large vehicle (e.g., a train) may have thickness $D \approx 1$ m and sound speed ≈ 330 m/s, and so a source frequency of greater than about just 1 kHz would give $k > 20$, for which parameter regime high-frequency asymptotics usually yield very good approximations.

Received Aug. 7, 1992; revision received June 22, 1993; accepted for publication June 23, 1993.

*Professor, Department of Mathematics.
†Professor, Department of Mathematics.
‡Professor, Department of Engineering Sciences and Applied Mathematics, The Technological Institute.

Rays emanating from the source carry energy (noise) from the source to the field. Some of this energy is either radiated directly to the far field away from the wall, or it is propagated upstream and then "turned" by the flow to the downstream far field. Furthermore, some of the energy is transmitted by the source rays directly to the wall and then reflected. Part of this reflected energy is then radiated to the far field. However, there are two one-parameter families of reflected rays that are trapped in a channel adjacent to the wall that do not escape to the far field. Each ray in this channel is alternately refracted toward the wall by the shear flow gradient and then reflected from the wall. These two families of rays then form an infinite sequence of caustics downstream of the source. Since caustics are curves along which the acoustic field intensity suddenly becomes large, they could dominate a distant signal received by a sensor located near a caustic.

The amplitude of the acoustic field from a line source was calculated in Kriegsmann and Reiss[5] by the method of geometrical acoustics. A boundary-layer method, similar to the one developed in Buchal and Keller[6] for the Helmholtz equation, was then employed to determine the acoustic amplitude on and near the caustics. Here we show that the amplitudes of the field on and near the caustics are $\mathcal{O}(k^{1/6})$ larger than the geometrical acoustics field away from the caustics for large k. Here k is the dimensionless wave number that is defined by $k = \omega D/c_0$, where c_0 is the ambient sound velocity in the shear layer, ω is the circular frequency of the time periodic component of the source, and D is the depth of the layer. More significantly, the vorticity of the acoustic field on and near the caustics is $\mathcal{O}(k^{2/3})$ larger than the vorticity of the geometrical acoustics field away from the caustics.

In Abrahams et al.[7] we considered the problem studied in Kriegsmann and Reiss[5] for a general piecewise continuous wall shear flow, and specific results were presented for a linear shear profile. A different asymptotic technique was used to solve the problem than that described earlier (Kriegsmann and Reiss[5]). An integral representation of the solution was obtained by using Fourier transform methods. Then the method of stationary phase was employed to obtain an asymptotic approximation of the solution. The approximation was obtained in terms of a pair of functions that satisfy a certain homogeneous second-order differential equation. These functions have been studied previously, for the linear shear profile, by Jones,[8] and their asymptotic form in the high-frequency limit is taken. This yields a pair of parametric equations whose solutions show that there is an infinite set of caustics inside the shear layer and downstream of the source, in agreement with results obtained by Kriegsmann and Reiss.[5] The virtue of the method is that it is not necessary to solve the ray equations numerically to determine the scattered field and the caustic curves.

In Abrahams et al.,[9] we have used this method to study the propagation of waves from a time-harmonic line source in a linear shear layer flowing above an elastic plate. Classical linear plate theory is employed in the analysis, including structural dissipation in the plate. We have found that, for certain ranges of the geometrical and physical parameters of the fluid, plate, and shear flow, it is possible because of the structural dissipation to significantly decrease the amplitude of the acoustic field on the caustic.

Thus, the analyses show that a localized disturbance, the line source of unit amplitude, can generate an array of narrow regions downstream of the source and surrounding each caustic in which the vorticity intensity is extremely large, in the acoustic approximation. Our conjecture is that these local regions of high-intensity vorticity may serve as nuclei for the "birth" of coherent fluid structures. That is, the process of coherent structure formation and hence of turbulence production in the boundary layer may be a self-induced phenomenon: old bursts give birth to new structures that are caused by acoustic focusing.

To further investigate this speculative conjecture, we consider in this paper the fully three-dimensional propagation of acoustic waves from a point source in the shear flow. The asymptotic method employed in Abrahams et al.[9] is used to study moving and stationary point sources. The resulting caustic surfaces form "structures" that are focused in a relatively narrow region. They are similar in appearance to the experimentally observed coherent fluid structures (see Sec. VIII). Since the amplitudes on the caustics are very large as $k \to \infty$, a nonlinear analysis may be required to describe the further evolution of the local vortex nuclei of the acoustic theory.

The purely acoustical implications of this work are well defined, as has been discussed earlier with reference to vehicle self-noise. However, the relevance of caustics (on which vorticity is large) in an inviscid model involving purely linear motions to coherent structures in a turbulent flow is far more controversial. The main aim of this work is to offer a physical mechanism for the production of regions, or surfaces, on which vorticity is high, and thus, for the "early-time" development of coherent structures, the assumption of linear disturbances seems reasonable. Obviously, the jitter associated with the time-varying nature of real sources in shear layers and with the defocusing effects of nonlinearity and viscosity means that our model can only be expected to hold for the earliest moments of a structure's development.

As with other models for wall region coherent structure dynamics, the viscous stresses in the laminar sublayer are not considered important here and are therefore ignored. It is assumed that the dominant effect of viscosity in the laminar sublayer is to impose the basic shear layer velocity profile. We believe that the effect of viscosity (and nonlinearity too) on the bounding of the caustic amplitude, and hence its vorticity, will be small. Popular models for early-time coherent structure development (e.g., Falco[4] and Smith et al.[10]) are based on the three-dimensional incompressible hydrodynamic interaction of asymmetric hairpin vortices with the background shear flow or with each other and are necessarily nonlinear in nature. The mechanism proposed in this article is therefore radically different. However, it is offered not as an alternative to the aforementioned but is instead complementary to it and adds another element that we believe is important; namely, compressibility. We show that compressibility leads to caustic formation from a point disturbance and hence to the creation of vortex surfaces of a particular characteristic shape. In contrast, the previous models that involve the distortion of hairpin vortices do not postulate the initial creation of these line vortices. Unfortunately, numerical simulations of turbulent wall or channel flows (e.g., Kim et al.[11]) do not find evidence of caustic formation to confirm this analytical investigation, but this is not at all surprising since almost all studies assume an incompressible fluid! With the previous limitations in mind, we proceed in the next section to define the boundary-value problem.

II. Formulation

We now formulate the three-dimensional acoustic problem for a time-harmonic point source in a two-dimensional shear flow of a compressible, inviscid fluid above a rigid plane. Cartesian coordinates (x, y, z) are defined such that x is the direction of flow, y is spanwise to the flow direction, and z is normal to the rigid plane at $z = 0$. The basic shear flow is given by

$$P = P_0, \quad \rho = \rho_0, \quad \boldsymbol{U} = \boldsymbol{U}_0 = (U_0(z), 0, 0) \tag{1}$$

where P_0 and ρ_0 are prescribed constant pressure and density, and the prescribed shear flow velocity is a specified one-dimensional vector with $U_0(z)$ defined by

$$U_0(0) = 0; \quad U_0(z) = U_\infty, \quad z \geq D$$
$$\frac{dU_0}{dz} \neq 0, \quad 0 \leq z \leq D \tag{2}$$

where U_∞ is the prescribed uniform flow at $z = \infty$, and D is the thickness of the shear layer. We observe that Eq. (1) is a solution of the equations of conservation of momentum and mass, which are given by

$$\frac{\partial \boldsymbol{U}}{\partial T} + (\boldsymbol{U} \cdot \nabla)\boldsymbol{U} = -\frac{1}{\rho}\nabla P \tag{3}$$

$$\frac{\partial \rho}{\partial T} + \nabla \cdot (\rho \boldsymbol{U}) = 0 \tag{4}$$

where T is time, ρ is density, P is pressure, $\boldsymbol{U}$ is the velocity vector, and the equation of state of the fluid is given by the following expression relating pressure and density:

$$\frac{dP}{d\rho} = c^2(\rho) \tag{5}$$

where $c^2(\rho)$ is the sound speed of the fluid. Thus Eqs. (3–5) are five scalar equations for the five scalar unknowns P, ρ, and $\boldsymbol{U}$.

The time-harmonic point mass source, say S, of circular frequency ω and small amplitude is at the point $x = y = 0$, $z = z_0 < D$, so that the point source is inside the shear layer. To study the propagation of small-amplitude acoustic waves from this point source, we linearize, with respect to the amplitude of the source, the solution of Eqs. (3–5) about the basic shear flow in Eq. (1) and get

$$\mathfrak{L}u + Mu_0'(z)\, w + \rho_x = 0 \tag{6}$$

$$\mathfrak{L}v + \rho_y = 0 \tag{7}$$

$$\mathfrak{L}w + \rho_z = 0 \tag{8}$$

$$\mathfrak{L}\rho + (u_x + v_y + w_z) = S(\boldsymbol{x}) \tag{9}$$

where we have factored out the harmonic time dependence $e^{i\omega T}$. In Eq. (6–9) we have used the notation $M \equiv \boldsymbol{U}_\infty/c_0$, where $c_0 \equiv c(\rho_0)$, so that M is a Mach number for the basic shear flow. The dimensionless density $\rho(\boldsymbol{x})$, velocity $\boldsymbol{u}(\boldsymbol{x}) = (u(\boldsymbol{x}), v(\boldsymbol{x}), w(\boldsymbol{x}))$, and coordinates $\boldsymbol{x} = (x, y, z)$ are obtained by dividing the corresponding dimensional quantities by $\rho_0 M$, $\boldsymbol{U}_\infty$, and D, respectively. Finally,

$$u_0(0) = 0; \quad u_0(z) = 1, \ z \geq 1; \quad u_0'(z) \neq 0, \ 0 \leq z \leq 1 \tag{10}$$

where $u_0'(z) \equiv du_0/dz$, and the differential operator $\mathfrak{L}$ is

$$\mathfrak{L} \equiv ik + u_0 M \frac{\partial}{\partial x} \tag{11}$$

where the wave number k is given by $k = \omega D/c_0$ and we also define a Strouhal number s as

$$s \equiv \omega D/\boldsymbol{U}_\infty = k/M \tag{12}$$

The pressure has been eliminated from Eqs. (6–8) by using the equation of state, Eq. (5).

We eliminate u and v from Eqs. (6–9) by differentiating Eqs. (6–8) with respect to x, y, and z, respectively, and adding the result to form $\mathfrak{L}(u_x + v_y + w_z)$. Then by substituting this result into Eq. (9), we obtain

$$\Delta\rho - \mathfrak{L}^2\rho + 2Mu_0' w_x = \delta(x)\delta(y)\delta(z - z_0) \tag{13}$$

where $\delta(x)\delta(y)\delta(z - z_0)$ is a stationary source function, $-\mathfrak{L}S(\boldsymbol{x})$, situated at $(0, 0, z_0)$. Here $\delta(x)$, etc., is the Dirac delta function, and S was introduced in Eq. (9). We will discuss the problem of a moving source in Sec. VII. Note that, as $M \to 0$, the operator $\mathfrak{L}$ tends to the value ik, and so Eq. (13) reduces to Helmholtz's equation for a stationary fluid.

Thus, the scattering problem that we consider consists of solving the coupled system of partial differential equations (8) and (13) for $w(x)$ and $\rho(x)$, subjected to the rigid surface condition

$$w(x, y, 0) = 0 \tag{14}$$

the radiation condition that waves are outgoing as

$$r = [x^2 + y^2 + z^2]^{1/2} \to \infty$$

and the conditions of continuity of $\rho(z)$ and $w(z)$ at $z = 1$.

III. Solution of the Scattering Problem for the Stationary Source

To solve the scattering problem defined in Sec. II, we first Fourier transform Eqs. (8) and (13) with respect to x and y to yield two ordinary differential equations in z for the Fourier transforms $\tilde{\rho}$ and $\tilde{w}$ of ρ and w, where the double Fourier transform is defined by

$$\tilde{\rho}(z;\xi,\eta) \equiv \int_{-\infty}^{\infty}\int_{-\infty}^{\infty} \rho(x, y, z) \exp(is[\xi x + \eta y])\, dx\, dy \tag{15}$$

and the inverse transform is defined by

$$\rho(x, y, z) \equiv \frac{s^2}{4\pi^2}\int_{-\infty}^{\infty}\int_{-\infty}^{\infty} \tilde{\rho}(z;\xi,\eta) \exp(-is[\xi x + \eta y])\, d\xi\, d\eta \tag{16}$$

The inclusion of s, the Strouhal number, in the previous exponents is purely for algebraic convenience. Then by eliminating $\tilde{w}$ from the two ordinary differential equations, we get, for $z < 1$,

$$\tilde{\rho}'' + \frac{2\xi u_0'(z)}{[1 - \xi u_0(z)]}\tilde{\rho}' + s^2\{[1 - \xi u_0(z)]^2 M^2 - \xi^2 - \eta^2\}\tilde{\rho} = \delta(z - z_0) \tag{17}$$

and in the constant velocity region, for $z > 1$,

$$\tilde{\rho}'' + s^2 Q^2 \tilde{\rho} = 0 \tag{18}$$

where the dash $'$ denotes differentiation with respect to z, and Q^2 is defined by

$$Q^2 \equiv M^2(1 - \xi)^2 - \xi^2 - \eta^2 \tag{19}$$

We shall consider subsonic shear flows, so that $M < 1$. Then the function $Q(\xi,\eta)$ is defined as having two branch cuts in the complex ξ plane; the cuts emanating from the branch points

$$[-M^2 \pm \sqrt{M^2 - (1 - M^2)\eta^2}\,]/(1 - M^2)$$

and going off to $\pm\infty$ along the positive and negative real axes, respectively. In the next sections it is shown that, for the particular solutions of interest, the values of η lie between $\pm M$. This ensures that the branch points of Q in the ξ plane always lie on the real line. For convenience, the Strouhal number is given a small negative imaginary part, Jones,[8] which allows the inverse integration path in Eq. (16) to pass just below the left-hand cut of Q and just above the right-hand cut. This further implies that the general solution of Eq. (18) that satisfies the outgoing radiation condition is, for $z > 1$,

$$\tilde{\rho}(z;\xi,\eta) = A(\xi,\eta)\exp[-isQ(z - 1)] \tag{20}$$

where $A(\xi, \eta)$ is to be determined and that branch of Q is chosen such that

$$Q(0, \eta) = +\sqrt{M^2 - \eta^2} \tag{21}$$

To solve Eq. (17) we define two independent solutions, which we denote by $f(z)$ and $g(z)$, of the homogeneous form of Eq. (17). The Wronskian of $f(z)$ and $g(z)$ may be given by

$$g(z)f'(z) - f(z)g'(z) = s^{2/3}[1-\xi u_0(z)]^2/\pi \tag{22}$$

as we can show. By satisfying the continuity conditions at $z = 1$ and discontinuity in the vertical velocity across the source, the solution is obtained as

$$\tilde{p}(z;\xi,\eta) = \frac{\pi A(\xi,\eta)}{s^{2/3}(1-\xi)^2}\{f'(1)g(z) - g'(1)f(z) + isQ[f(1)g(z) - g(1)f(z)]\} \tag{23}$$

in $z_0 \le z \le 1$, where

$$A(\xi,\eta) = \frac{g'(0)f(z_0) - f'(0)g(z_0)}{\{f'(0)g'(1) - g'(0)f'(1) + isQ[f'(0)g(1) - g'(0)f(1)]\}} \frac{(1-\xi)^2}{[1-\xi u_0(z_0)]^2} \tag{24}$$

The result for $z > 1$ is given by employing expression (24) in Eq. (20). For $z < z_0$, Eqs. (23) amd (24) are valid if z and z_0 are interchanged everywhere in the numerators.

IV. Asymptotic Representation of the Solution for Large Strouhal Number

The limit of large Strouhal number s is by Eq. (12) equivalent to $k \to \infty$ for fixed M. Asymptotic approximations for the two solutions f and g of Eq. (17) are obtained by using turning point theory, Olver,[12] as

$$f(z) \sim [1-\xi u_0(z)]\{\zeta(z)/q^2(z)\}^{1/4}\,\mathrm{Ai}[-s^{2/3}\zeta(z)] \tag{25}$$

$$g(z) \sim [1-\xi u_0(z)]\{\zeta(z)/q^2(z)\}^{1/4}\,\mathrm{Bi}[-s^{2/3}\zeta(z)] \tag{26}$$

where it has been assumed that $\xi < 1$, $\mathrm{Ai}(x)$, and $\mathrm{Bi}(x)$ are Airy functions of the first and second kind, $q(z)$ is defined by

$$q^2(z) \equiv M^2[1-\xi u_0(z)]^2 - (\xi^2+\eta^2) \tag{27}$$

and

$$\zeta(z) \equiv \left|\frac{3}{2}\int q(z)\,dz\right|^{2/3} \tag{28}$$

for $q^2(z) > 0$, or

$$\zeta(z) \equiv -\left|\frac{3}{2}\int [-q^2(z)]^{1/2}\,dz\right|^{2/3} \tag{29}$$

for $q^2(z) < 0$. Note that $q(1) = Q$. For a linear shear profile, $u_0(z) \equiv z$, the integrals can be evaluated explicitly as

$$\zeta(z) \equiv \left|\frac{3}{4\xi}[1-\xi u_0(z)]\,q(z) - \frac{3(\xi^2+\eta^2)}{4\xi M} \times \cosh^{-1}\left\{\frac{[1-\xi u_0(z)]M}{\sqrt{\xi^2+\eta^2}}\right\}\right|^{2/3} \tag{30}$$

for $q^2(z) > 0$,

$$\zeta(z) \equiv -\left|\frac{3}{4\xi}[1-\xi u_0(z)]\,[-q^2(z)]^{1/2} - \frac{3(\xi^2+\eta^2)}{4\xi M} \times \cos^{-1}\left\{\frac{[1-\xi u_0(z)]M}{\sqrt{\xi^2+\eta^2}}\right\}\right|^{2/3} \tag{31}$$

for $q^2(z) < 0$. We will confine our attention to the linear profile in the numerical investigation to follow.

The method of stationary phase is now employed to evaluate the inverse transform integral of Eq. (16). The sound field inside the shear layer downstream of the source is of particular interest. From previous work (Abrahams et al.[7]) the stationary phase points are expected to lie just above the right-hand branch of Q, between the branch point and the smaller of $r(z)$, or $r(z_0)$, where $r(z)$ is defined by

$$r(z) \equiv \frac{-u_0(z)M^2 + \sqrt{M^2 - [1-u_0^2(z)M^2]\eta^2}}{1-u_0^2(z)M^2} \tag{32}$$

Thus the points of interest lie to the right of $r(1)$ (the branch point of Q), and so $q^2(1)$ is negative. Hence the arguments of the Airy functions in $f(1)$ and $g(1)$ are positive in sign, and so $f(1)$ and $f'(1)$ are exponentially small and are neglected with respect to $g(1)$ and $g'(1)$, which are exponentially large. This approximation is employed in Eq. (23) to yield, where $1 > z > z_0$,

$$\tilde{p}(z;\xi,\eta) \underset{s\to\infty}{\sim} \frac{\pi f(z)\,[f'(0)g(z_0) - g'(0)f(z_0)]}{[1-\xi u_0(z_0)]^2 s^{2/3} f'(0)} \tag{33}$$

The Airy functions appearing in the remaining f and g all have negative argument and can therefore be represented by oscillatory terms, giving

$$\tilde{p}(z;\xi,\eta) \underset{s\to\infty}{\sim} \frac{[1-\xi u_0(z)]}{[1-\xi u_0(z_0)]} \frac{[q(z)q(z_0)]^{-1/2}}{s} \times \frac{\sin[s\alpha(z) + \pi/4]}{\cos[s\alpha(0) + \pi/4]} \cos[s\alpha(0) - s\alpha(z_0)] \tag{34}$$

for $1 > z > z_0$ in the shear layer with $\alpha(z)$ defined by

$$\alpha(z) \equiv (2/3)\zeta^{3/2}(z) \tag{35}$$

The presence of the oscillatory term in the denominator of Eq. (34) is due to the repeated reflection and refraction of some of the rays emanating from the source as they travel downstream. Thus, any point inside the shear layer and downstream of the source may have many rays contributing to the sound field. Each separate ray will have a particular stationary phase point in the complex ξ and η planes, and to determine these points we rewrite

$$\sec[s\alpha(0) + \pi/4] = 2\exp[-is\alpha(0) - \pi i/4] \times \sum_{N=0}^{\infty} \exp[N\pi i/2 - 2iNs\alpha(0)] \tag{36}$$

where the infinite sum formally converges because of the small negative imaginary part of s. The asymptotic approximation of the

solution is now written as a sum of stationary phase integrals, for $1 > z > z_0$, namely,

$$\rho(x, y, z) \underset{s\to\infty}{\sim} \sum_{j,\ \ell=0}^{1} \sum_{N=0}^{\infty} \int_{-\infty}^{\infty}\int_{-\infty}^{\infty} s\Lambda_\ell(\xi, \eta)\, e^{ish(\xi,\eta)}\, d\xi\, d\eta \quad (37)$$

with $\Lambda_\ell(\xi, \eta)$ defined by

$$\Lambda_\ell(\xi, \eta) \equiv \frac{[1-\xi u_0(z)]}{8\pi^2[1-\xi u_0(z_0)]} \frac{\exp[i\pi(N+\ell-1)/2]}{[q(z)q(z_0)]^{1/2}} \quad (38)$$

over the significant part of the (ξ, η) space, and $h(\xi, \eta)$ given as

$$h(\xi, \eta) = (-1)^\ell \alpha(z) + (-1)^j \alpha(z_0) - [2N + 1 + (-1)^j]\alpha(0) - \xi x - \eta y \quad (39)$$

For $z < z_0$ the density is given by Eq. (37) if z and z_0 are interchanged in Eq. (39).

At any point (x, y, z) a contribution is made to the sound field from the (j, ℓ, N)th integral if a stationary phase point (ξ^*, η^*), say, lies in the interval

$$r(1) < \xi^* < \min[r(z), r(z_0)], \qquad |\eta^*| < M \quad (40)$$

where $r(z)$ is given in Eq. (32). At this point the gradient, $\nabla \equiv (\partial/\partial\xi, \partial/\partial\eta)$, of the argument of the exponent vanishes,

$$\nabla h(\xi^*, \eta^*) = \mathbf{0} \quad (41)$$

so that a Taylor's series expansion yields

$$h(\xi, \eta) \approx h^* + (1/2)\,[(\xi-\xi^*)^2 h^*_{\xi\xi} + 2(\xi-\xi^*)(\eta-\eta^*)h^*_{\xi\eta} + (\eta-\eta^*)^2 h^*_{\eta\eta}] \quad (42)$$

in which $h^* \equiv h(\xi^*, \eta^*)$, and $h^*_{\xi\eta}$ is the second derivative of $h(\xi, \eta)$ with respect to ξ and η evaluated at (ξ^*, η^*), etc. A numerical study has demonstrated that sufficiently far upstream inside the shear layer there are no contributory terms (shadow region). Nearer to the source and upstream of it, there is a single term in the $\ell = 0$ sum that has a stationary phase contribution. However, for any point lying in a region $y < y_{\max}$ downstream, there are a finite number of terms when $\ell = 0$. Here, $y_{\max}$ is defined in Eq. (65). For any term in the sum, denoted by $\rho_{j\ell N}$, which satisfies the aforementioned criteria, the integral may be approximated by

$$\rho_{j\ell N} \sim s\Lambda_\ell(\xi^*, \eta^*) e^{ish^*} \int_{-\infty}^{\infty}\int_{-\infty}^{\infty} e^{(1/2)is\underline{\xi}\boldsymbol{A}\underline{\xi}^T} d\xi\, d\eta \quad (43)$$

where $\underline{\xi} = (\xi-\xi^*, \eta-\eta^*)$, $\underline{\xi}^T$ denotes the transpose of $\underline{\xi}$, and $\boldsymbol{A}$ is the square matrix

$$\boldsymbol{A} = \begin{pmatrix} h^*_{\xi\xi} & h^*_{\xi\eta} \\ h^*_{\eta\xi} & h^*_{\eta\eta} \end{pmatrix} \quad (44)$$

The double integral is evaluated by introducing new variables p_1 and p_2 such that

$$(p_1, p_2) = (\xi-\xi^*, \eta-\eta^*)\boldsymbol{X} \quad (45)$$

where

$$\boldsymbol{X}\begin{pmatrix} \lambda_+ & 0 \\ 0 & \lambda_- \end{pmatrix}\boldsymbol{X}^T = \boldsymbol{A} \quad (46)$$

or

$$\boldsymbol{X} = \begin{pmatrix} h^*_{\xi\eta} & -\Theta \\ \Theta & h^*_{\xi\eta} \end{pmatrix}\Delta^{-1/2} \quad (47)$$

and

$$\lambda_\pm = \left[h^*_{\xi\xi} + h^*_{\eta\eta} \pm \sqrt{(h^*_{\xi\xi} - h^*_{\eta\eta})^2 + 4h^{*2}_{\xi\eta}}\right]/2 \quad (48)$$

$$\Theta = \lambda_- + h^*_{\eta\eta}, \qquad \Delta = h^{*2}_{\xi\eta} + \Theta^2 \quad (49)$$

Substitution into Eq. (43) gives

$$\rho_{\ell jN} \underset{s\to\infty}{\sim} s\Lambda_\ell(\xi^*, \eta^*) e^{ish^*} \int_{-\infty}^{\infty} e^{is\lambda_+ p_1^2} dp_1 \int_{-\infty}^{\infty} e^{is\lambda_- p_2^2} dp_2 \quad (50)$$

since the Jacobian of the transformation has a value of unity. The total sound field is thus composed of a sum of terms of the form

$$\rho_{\ell jN} \underset{s\to\infty}{\sim} \pi\Lambda_\ell(\xi^*, \eta^*) e^{ish^*} e^{-i\pi/2} / (\lambda_+\lambda_-)^{1/2} \quad (51)$$

where

$$(\lambda_+\lambda_-) = h^*_{\xi\xi}h^*_{\eta\eta} - h^{*2}_{\xi\eta} = \|\boldsymbol{A}\| \quad (52)$$

V. Sound Field on a Caustic

The caustics of the sound field are surfaces, which are envelopes of the rays, and are characterized in the complex (ξ, η) planes by a coalescence of stationary points. Thus, the amplitude of the acoustic field and, in particular, the amplitude of the acoustic vorticity field are much larger on the caustic surfaces than off these surfaces. The surfaces are obtained by requiring that at (ξ^*, η^*) both

$$\nabla h = \mathbf{0} \quad (53)$$

and

$$\|\boldsymbol{A}\| = 0 \quad (54)$$

It can be shown that there are two families of caustics, which we denote as caustic families F1 and F2, respectively, one given for $\ell = 0, j = 0$ for $N \geq 0$, the other satisfying $\ell = 0, j = 1$ for $N \geq 0$. On a caustic, one of the eigenvalues, λ_-, vanishes so that $\Theta = h^*_{\eta\eta}$,

$$\lambda_+ = h^*_{\xi\xi} + h^*_{\eta\eta} \quad (55)$$

and

$$\Delta = h^*_{\eta\eta}(h^*_{\xi\xi} + h^*_{\xi\eta}) \quad (56)$$

Equation (51) is invalid under these circumstances because the denominator is zero. The next term of the Taylor's series expansion Eq. (42) is thus included to yield

$$\rho_{0jN} \underset{s\to\infty}{\sim} s\Lambda_0(\xi^*, \eta^*) e^{ish^*} \int_{-\infty}^{\infty} e^{is\lambda_+ p_1^2}\, dp_1 \int_{-\infty}^{\infty} e^{isH\lambda_+^{-3/2}p_2^3}\, dp_2$$

$$= \frac{2s^{1/6}\sqrt{\pi}}{3H^{1/3}}\Gamma(1/3)\cos(\pi/6)\,\Lambda_0(\xi^*, \eta^*)\, e^{i(sh^* - \pi/4)} \quad (57)$$

where

$$H = \left|h^*_{\eta\eta}\right|^{-3/2} \times \left|h^*_{\xi\xi\xi}h^{*3}_{\eta\eta} - 3h^*_{\xi\xi\eta}h^{*2}_{\eta\eta}h^*_{\xi\eta} + 3h^*_{\xi\eta\eta}h^*_{\eta\eta}h^{*2}_{\xi\eta} - h^*_{\eta\eta\eta}h^{*3}_{\xi\eta}\right|/6 \quad (58)$$

We observe that the sound field on a caustic is $\mathcal{O}(s^{1/6})$ as $s \to \infty$ rather than the $\mathcal{O}(1)$ value everywhere else in the acoustic field [see Eq. (51)]. We recall that the field is $\mathcal{O}(s^{-1/2})$ as $s \to \infty$ away from the caustics for a line source, as considered in Abrahams et al.,[7] and Kriegsmann and Reiss,[5] and it is $\mathcal{O}(1)$ for the point source considered in this paper.

The three scalar equations, Eqs. (53) and (54), define the caustic surfaces, and for given N and z_0 values the stationary phase points (ξ^*, η^*) are used parametrically to numerically determine x and y. We now illustrate these surfaces for the linear shear profile $u_0(z) \equiv z$. Figure 1 shows a section through the first five caustics ($N = 1, \ldots, 5$) of the F1 family at $z = 0.8$ for the parameter values $M = 0.7$, and $z_0 = 0.5$. Figure 2 shows the first three caustics of both families (F2 are dashed) for the same parameter values as in Fig. 1. Only half of each caustic is shown because of the symmetry about the x axis. Figures 3a and 3b illustrate the two different caustic surfaces over the whole height of the shear layer.

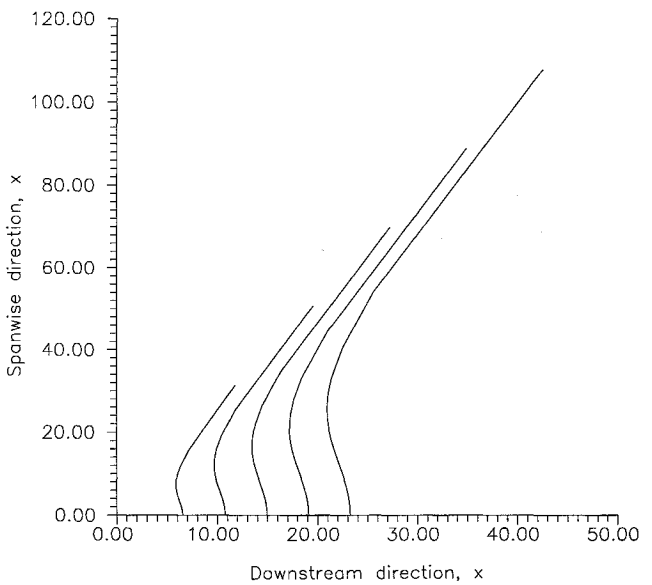

Fig. 1 Level curves of caustic surfaces at $z = 0.8$ for caustic family F1, for $N = 1, 2, 3, 4, 5$. Here, and in all subsequent figures, the source is located at $z_0 = 0.5$.

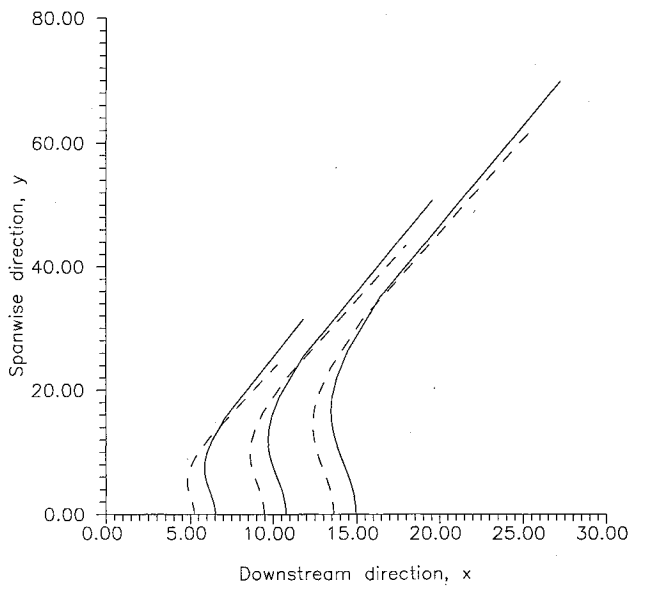

Fig. 2 Level curves of caustic surfaces at $z = 0.8$ for F1, for $N = 1, 2, 3$ (solid curves), and for F2, for $N = 1, 2, 3$ (dashed curves).

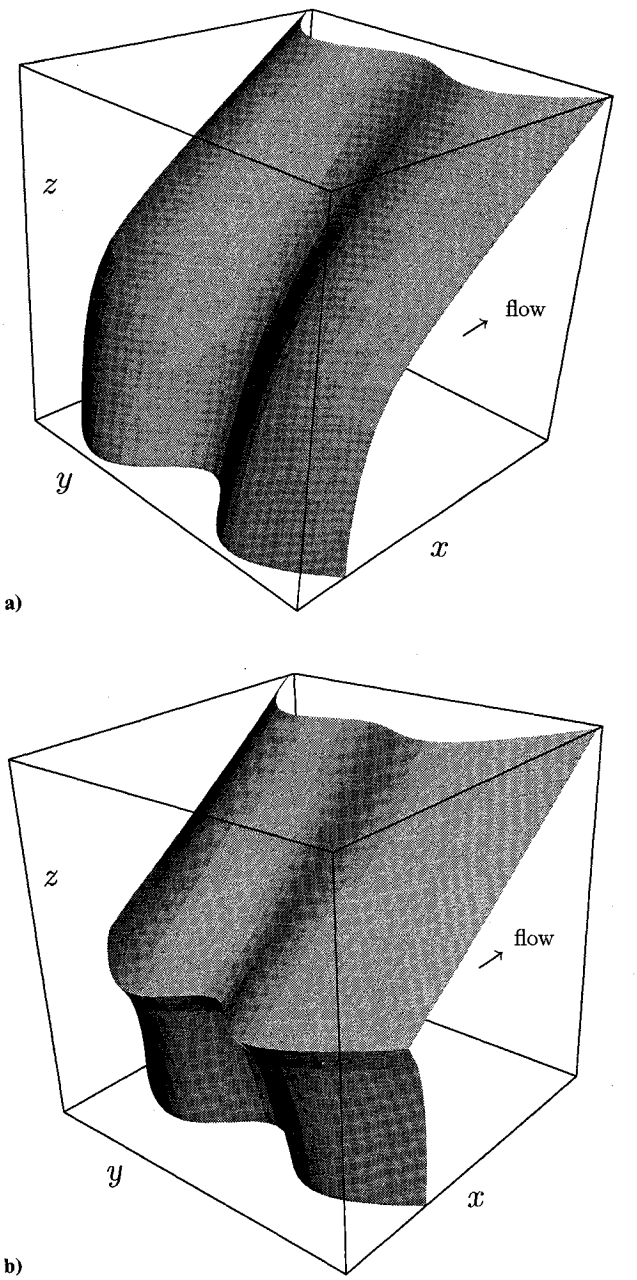

Fig. 3 For $N = 1$: a) caustic surface of family F1 and b) caustic surface of family F2.

VI. Asymptotic Approximation of the Solution near the Caustic Edge

It is suggested by the results shown in Fig. 1 that if the caustics were extended indefinitely away from the x axis, then they would all asymptote to the same line. This is the path of the outermost ray (viewed from above), that undergoes continuous reflections and refractions downstream. For any point on this "tail" of the caustic, we perform an additional asymptotic analysis to simplify Eqs. (53) and (55) and hence ease the calculation of the order of magnitude of the sound field. On the tail we find numerically that one of the complex variables, η^*, approaches its limiting value M. Hence a suitable small parameter ε is defined by

$$\eta = M(1 - \varepsilon), \qquad \varepsilon \to 0 \tag{59}$$

where the strict ordering $\varepsilon >> 1/s^2$ must be preserved. To simplify the presentation the superscript * is omitted from η and ξ in the fol-

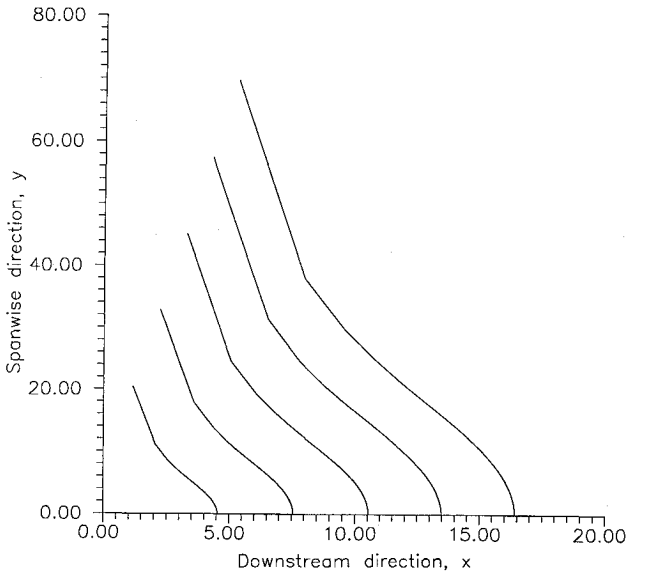

Fig. 4 Level curves of caustic surfaces at $z = 0.8$ for F1, for $N = 1, 2, 3, 4, 5$, and a moving source with velocity $V = 0.5\ U_\infty$ where U_∞ is flow velocity at $z = \infty$.

lowing analysis. By substituting Eq. (59) into Eq. (40), we obtain the interval for ξ, when $1 > z > z_0$, as

$$\varepsilon < \xi < \varepsilon/z \tag{60}$$

and so the new variable

$$\nu = \xi/\varepsilon \tag{61}$$

has the range, for $1 > z > z_0$,

$$1 < \nu < 1/z \tag{62}$$

These new parameters ε and ν are introduced into the caustic equations in the the Appendix, but the resultant expression, Eq. (A5), must still be calculated numerically to obtain the caustic path. If, however, the asymptotic form of the tail is sought on a distant caustic (N large but $N << 1/\varepsilon$) then the stationary value of ν can be obtained explicitly. This is performed in Eq. (A7), and the asymptote for any caustic is found to be [see Eqs. (A9–A11)], for $z > z_0$,

$$y \sim \sqrt{(2/\varepsilon)}\, z\, [2N \mp \sqrt{1 - z_0/z} + \mathcal{O}(N^{-1})] \tag{63}$$

$$x \sim \sqrt{(2/\varepsilon)}\, Mz^2\, [4N \mp (2 + z_0/z)\sqrt{1 - z_0/z} + \mathcal{O}(N^{-1})]/3 \tag{64}$$

and so

$$y = y_{\max} = 3x\, [1 \pm z_0\sqrt{1 - z_0/z}/(4Nz) + \mathcal{O}(N^{-2})]/(2Mz) \tag{65}$$

where the upper and lower signs belong to the F1 and F2 caustic families, respectively. Equations (63–65) are, for simplicity, presented for a linear shear profile $u_0(z) \equiv z$, and also hold for $z < z_0$ if z and z_0 are interchanged.

The magnitude of the sound field can also be estimated on the extreme portion of the caustic. By using Eq. (A1) and Eqs. (A12–A15) it is found that

$$q(z) \sim \mathcal{O}(\varepsilon^{1/2}), \qquad h^*_{\xi\xi} \sim h^*_{\eta\xi} \sim h^*_{\eta\eta} \sim \mathcal{O}(\varepsilon^{-3/2}) \tag{66}$$

$$h^*_{\xi\xi\xi} \sim h^*_{\xi\xi\eta} \sim h^*_{\xi\eta\eta} \sim h^*_{\eta\eta\eta} \sim \mathcal{O}(\varepsilon^{-5/2}) \tag{67}$$

and so

$$H \sim \mathcal{O}(\varepsilon^{-19/4}), \qquad \Lambda_0 \sim \mathcal{O}(\varepsilon^{-1/2}) \tag{68}$$

Hence, from Eq. (57), the magnitude of the sound field decays as

$$\rho(x, y, z) \sim \mathcal{O}(\varepsilon^{13/12}) \sim \mathcal{O}(y^{-13/6}), \qquad y \to \infty \tag{69}$$

along a caustic away from the x axis. Note that this result holds for all shear profiles, not just the linear one illustrated.

VII. Moving Source

It is useful to extend the problem outlined in Sec. II to the radiation by a source moving with a constant velocity V, $V < U_\infty$, in the positive x direction. By repeating the previous analysis, the solu-

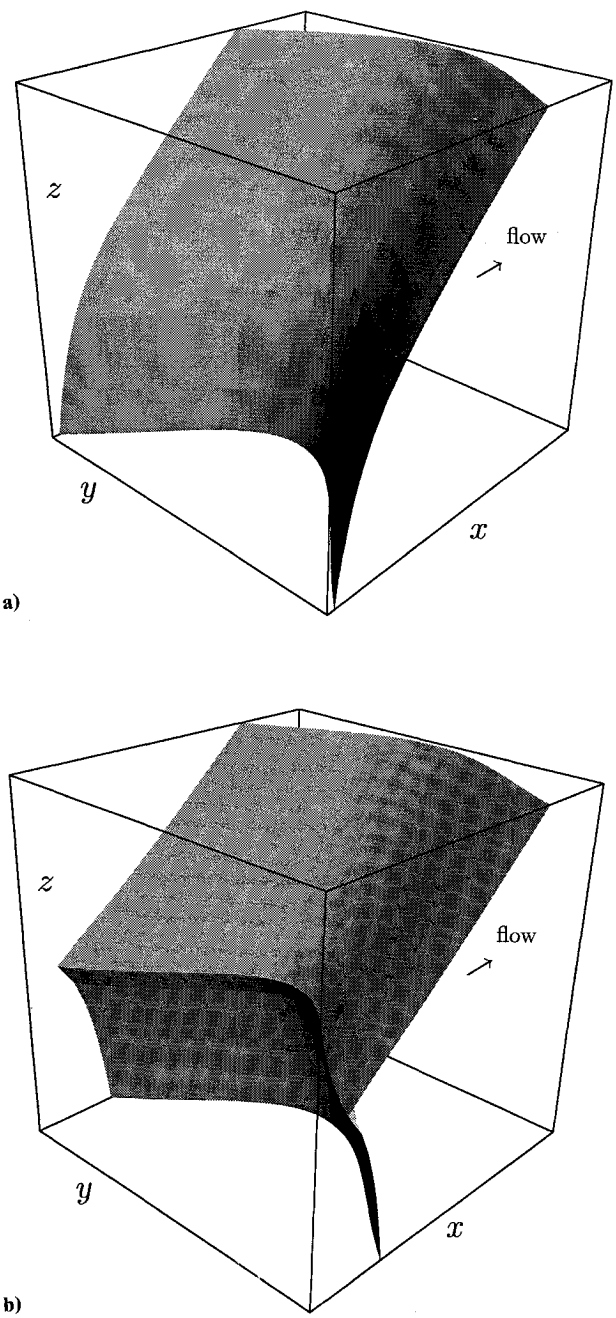

Fig. 5 For moving source with $N = 1$ and $V = 0.5\ U_\infty$: a) caustic surface of F1 and b) caustic surface of F2.

tion, in the large Strouhal limit, is again given by Eq. (37), for $1 > z > z_0$, as

$$\rho(x, y, z) \underset{s\to\infty}{\sim} \sum_{j,\,\ell=0}^{1} \sum_{N=0}^{\infty} \int_{-\infty}^{\infty}\int_{-\infty}^{\infty} s\Lambda_\ell(\xi,\eta)\, e^{ish(\xi,\eta)}\, d\xi\, d\eta \tag{70}$$

but now Λ_ℓ and $h(\xi, \eta)$ are defined by

$$\Lambda_\ell(\xi,\eta) \equiv \frac{[1-\xi u_0(z)]}{8\pi^2[1-\xi u_0(z_0)]} \frac{\exp[i\pi(N+\ell-1)/2]}{[\hat{q}(z)\hat{q}(z_0)]^{1/2}} \tag{71}$$

in which

$$\hat{q}^2(z) \equiv M^2\{1-\xi(u_0(z)-\sigma)\}^2 - (\xi^2+\eta^2) \tag{72}$$

$$\sigma \equiv V/U_\infty \tag{73}$$

and

$$h(\xi,\eta) = (-1)^\ell\, \hat{\alpha}(z) + (-1)^j \hat{\alpha}(z_0) - [2N+1+(-1)^j]\hat{\alpha}(0) - \xi[(x-x_0) - (t-t_0)\sigma] - \eta y \tag{74}$$

$$\hat{\alpha}(z) \equiv (2/3)\hat{\zeta}^{3/2}(z) \equiv \int \hat{q}(z)\, dz, \qquad \hat{q}^2(z) > 0 \tag{75}$$

where t is the dimensionless time $t \equiv U_\infty T/D$, and it is assumed that the source is at $(x_0, 0, z_0)$ at time t_0. The solution given in Sec. IV for any point on a ray, Eq. (51) and also the solution on a caustic, Eq. (57), are similarly valid using Eqs. (71) and (74), except that the stationary phase point (ξ^*, η^*) changes. This point can be shown to lie in the new interval

$$r_1(1) < \xi^* < \min[r_1(z), r_1(z_0)], \qquad |\eta^*| < M \tag{76}$$

where $r_1(z)$ is defined by

$$r_1(z) \equiv \frac{-[u_0(z)-\sigma]M^2 + \sqrt{M^2 - \{1-[u_0(z)-\sigma]M^2\}\eta^2}}{1-[u_0(z)-\sigma]^2 M^2} \tag{77}$$

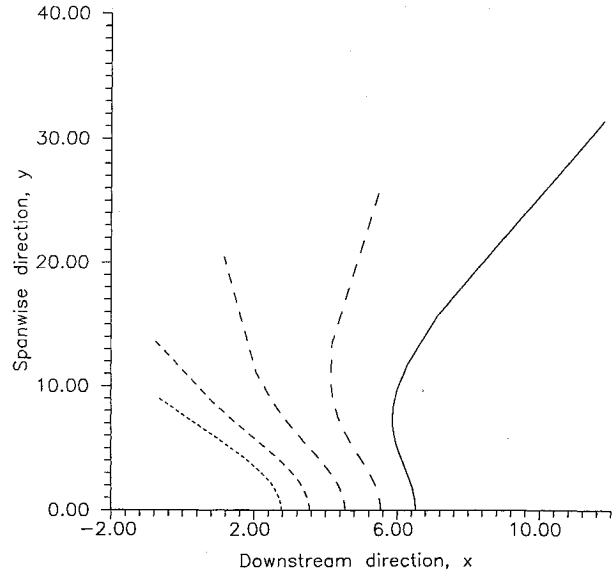

Fig. 6 Level curves of caustic surfaces at $z = 0.8$ for F1, for $N = 1$, and for moving sources with $\sigma = 0$ (solid line), 0.25, 0.5, 0.75, 0.95 (fine dashed line).

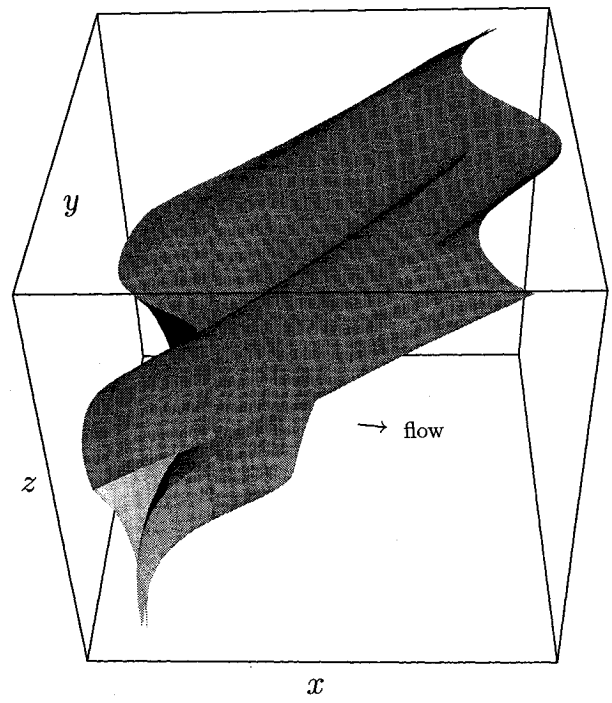

Fig. 7 Caustic surfaces of F1 ($N = 1$) and F2 ($N = 1$) for moving source with velocity $V = 0.2\ U_\infty$. Source is moving left to right in the direction of the flow.

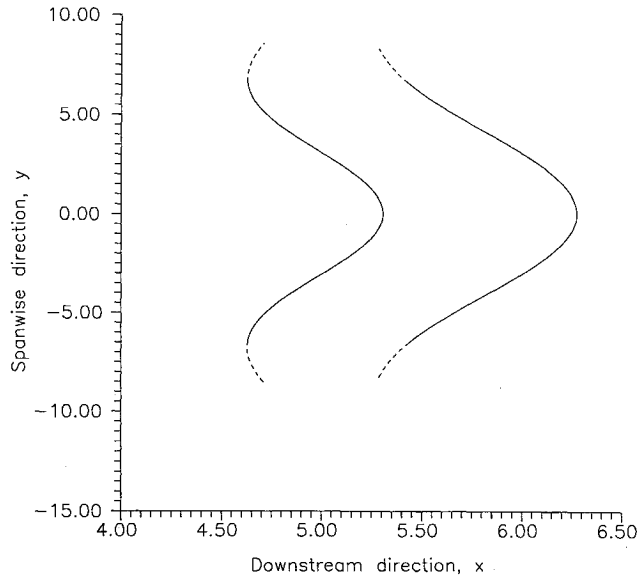

Fig. 8 Level curves, $z = 0.91$, of caustic surfaces shown in Fig. 7. Dashed line indicates that the amplitude has decayed to roughly 1% of that at the center of the caustic.

For a linear shear layer, Fig. 4 illustrates a section of the first five caustics of the F1 family for the same parameter values as in Fig. 1, and for the ratio, $\sigma = 0.5$. The caustics are viewed in a frame of reference that is stationary with respect to the source, and the source is placed at the origin. It is interesting to note how the caustics are "swept back" by the moving source. Figure 4 clearly shows this change from the stationary source pattern (Fig. 1), and the whole of the $N = 1$ caustic surfaces of families F1 and F2 are illustrated in Fig. 5. The effect of increasing V is illustrated in Fig. 6, and of special importance is the point on the caustic at which the sound field has decayed to a low level. We can show that the energy on a caustic surface becomes more localized (con-

fined around the central region near the x axis) as the source speed V increases. To illustrate this, the three-dimensional caustic surfaces shown in Figs. 3, 5, and 7 are cut off at an energy value of a few percent of that at the source point. The moving source caustics are cut off before dx/dy becomes positive on the surfaces.

VIII. Concluding Remarks

Finally, we consider the caustic surfaces of family F1, $N = 1$, and F2, $N = 1$, that are generated by a point source located at $z_0 = 0.5$ and moving with velocity $V = 0.2U_\infty$ left to right with $M = 0.695$ as shown in Fig. 7. Again the velocity profile of the imposed shear flow is linear. The surface has been deleted roughly where the amplitude of the caustic field is around 0.3% of its maximum value. The volume *between* the two surfaces can be compared with the experimentally determined turbulent spot moving in a laminar boundary layer, see e.g., Fig. 5 in Cantwell et al.[13] This may be easier for the reader to see by looking at the cross section through the surfaces at an arbitrary z station, say, $z = 0.91$ as shown in Fig. 8. The visual agreement between the experimentally and theoretically determined spots is remarkable, especially since we are using a linear theory to describe the initial formation of the spot. Notice the concave leading and convex trailing edges of both of the "heart-shaped" spots.

This paper has been concerned with the calculation and prediction of three-dimensional surfaces in a wall shear flow on which the vorticity is large, produced by high-frequency sources. Within the limitations of linear, inviscid theory, the results are exact. However, we suggest tentatively that this work may also act as a simple paradigm for the early-time development of coherent structures in the laminar sublayer of turbulent wall flows. Arguments were presented in the Introduction as to why our model, which neglects time-dependent features of the sources, viscous stresses, and nonlinearity, may nevertheless offer surfaces of high vorticity, which act as the "seeds" on which the unstable coherent structures form. Indeed, none of these three physical features will destroy the surfaces; they will only modify their shapes and limit the vorticity. We consider that the strong qualitative agreement illustrated earlier between our predictions and the experimentally observed coherent structures is encouraging and justifies further experimental and theoretical corroborative work to attempt a quantitative comparison. This is being initiated by the authors. As a final remark, we note that our work may also offer a mechanism for the formation of streamwise streaks that are observed in the sublayer of turbulent shear flows (Smith and Metzler[14]). These streaks, when contrasted with the shape of the distant regions of the caustic surfaces, again yield close visual agreement.

Appendix: Asymptotes of the Caustics

Here we determine the surface to which the tail of a distant caustic is asymptotic. Results are presented, for brevity, for the linear shear $u_0(z) \equiv z$, but the method is easily reproduced for any profile.

By substituting the new variables ε and ν, defined in Eqs. (59) and (61), into Eq. (27), we get

$$q^2(z) \sim 2\varepsilon M^2(1 - \nu z) \tag{A1}$$

and $\alpha(z)$ is approximated by

$$\alpha(z) \sim 2M\sqrt{2\varepsilon}\,(1-\nu z)^{3/2}/(3\nu) \tag{A2}$$

Then inserting these values in $h(\xi, \eta)$, Eq. (39), gives from Eq. (25) the asymptote

$$y \sim -\sqrt{2/\varepsilon}\,(\sqrt{1-\nu z} \pm \sqrt{1-\nu z_0} - 2N)/\nu \tag{A3}$$

$$x \sim -\sqrt{2/\varepsilon}\,M[(2+\nu z)\sqrt{1-\nu z} \pm (2+\nu z_0)\sqrt{1-\nu z_0} - 4N]/(3\nu^2) \tag{A4}$$

To determine the stationary phase point (ν, ε), it is necessary to find the second derivative terms of $\alpha(z)$ and then to substitute them into the expression $\|A\| = 0$. This gives, from Eq. (54), for $1 > z > z_0$,

$$\left[\frac{8-4\nu z-\nu^2 z^2}{(1-\nu z)^{1/2}} \pm \frac{8-4\nu z_0-\nu^2 z_0^2}{(1-\nu z_0)^{1/2}} - 16N\right] \times \left[\frac{1}{(1-\nu z)^{1/2}} \pm \frac{1}{(1-\nu z_0)^{1/2}} - N\right] - 3\left[\frac{(2-\nu z)}{(1-\nu z)^{1/2}} \pm \frac{(2-\nu z_0)}{(1-\nu z_0)^{1/2}} - 4N\right]^2 = 0 \tag{A5}$$

where z and z_0 are interchanged if $z < z_0$. For given z, z_0, and N, this equation must still be solved numerically to calculate ν, which is then used in Eqs. (A3) and (A4). However, the expression (A5) is further simplified by studying the asymptotic solution for large N, maintaining the ordering

$$1/N >> \varepsilon >> s^{-2} \tag{A6}$$

In this limit ν tends to its limit point $\nu \to 1/z$ for $z > z_0$, $\nu \to 1/z_0$ for $z < z_0$, and so the first term in each of the brackets of Eq. (A5) becomes large. Balancing the leading-order terms gives

$$32N \sim \frac{24 - 20\nu z + \nu^2 z^2}{(1-\nu z)^{1/2}} \tag{A7}$$

which gives

$$\nu \sim (1/z)\{1 - [5/(32N)]^2 + \mathcal{O}(N^{-3})\} \tag{A8}$$

Finally, the equations for the asymptotes, Eq. (A3) and (A4) are reduced, for $1 > z > z_0$, to

$$y \sim -\sqrt{2/\varepsilon}\,[\pm\sqrt{1-z_0/z} - 2N + \mathcal{O}(1/N)]z \tag{A9}$$

$$x \sim -\sqrt{2/\varepsilon}\,M[\pm(2+z_0/z)\sqrt{1-z_0/z} - 4N + \mathcal{O}(1/N)]z^2/3 \tag{A10}$$

and the surface slope, for $1 > z > z_0$, is given by

$$y \sim \frac{3x}{2Mz}\left[1 \pm \frac{z_0}{4Nz}\sqrt{1-z_0/z} + \mathcal{O}(1/N^2)\right] \tag{A11}$$

where again z and z_0 are interchanged for $z < z_0$. The upper and lower signs in Eqs. (A9–A11) correspond to the $j = 0$ and $j = 1$ caustic families, respectively.

The magnitude of the sound field on the tail of the caustic can be estimated by employing the results in this Appendix. We deduce from Eq. (A1) that $q(z)$ is of order $\varepsilon^{1/2}$ and from Eq. (38) that

$$\Lambda_0(\xi, \eta) \sim \mathcal{O}(\varepsilon^{-1/2}) \tag{A12}$$

The second derivative terms of α are all of order $\varepsilon^{-3/2}$, as we can show, and so

$$h^*_{\xi\xi} \sim h^*_{\xi\eta} \sim h^*_{\eta\eta} \sim \mathcal{O}(\varepsilon^{-3/2}) \tag{A13}$$

Similarly, differentiating again reveals that

$$h^*_{\xi\xi\xi} \sim h^*_{\xi\xi\eta} \sim h^*_{\xi\eta\eta} \sim h^*_{\eta\eta\eta} \sim \mathcal{O}(\varepsilon^{-5/2}) \tag{A14}$$

and so H, Eq. (58), attains the magnitude

$$H \sim \mathcal{O}(\varepsilon^{-19/4}) \tag{A15}$$

Acknowledgments

This work was supported in part by the Air Force Office of Scientific Research under Grant AFOSR-91-0252 and by the Office of Naval Research under Grant N00014-92-J-1261.

References

[1]Bushnell, D. M., Hefner, J. M., and Ash, R. L., "Effect of Compliant Wall Motion on Turbulent Boundary Layers," *Physics of Fluids*, Vol. 20, No. 10, Pt. II, 1977, pp. S31–S48.

[2]Cantwell, B. T., "Organized Motions in Turbulent Flow," *Annual Reviews of Fluid Mechanics*, Vol. 13, 1981, pp. 457–515.

[3]Offen, C. R., and Kline, S. J., "A Proposed Model of the Bursting Process in Turbulent Boundary Layers," *Journal of Fluid Mechanics*, Vol. 70, No. 2, 1975, pp. 209–228.

[4]Falco, R. E., "A Coherent Structure Model of the Turbulent Boundary Layer and its Ability to Predict Reynolds Number Dependence," *Philosophical Transactions of the Royal Society of London*, Series A: Mathematical and Physical Sciences, Vol. 336, No. 1641, 1991, pp. 103–129.

[5]Kriegsmann, G. A., and Reiss, E. L., "Acoustic Propagation in Wall Shear Flows and the Formation of Caustics," *Journal of the Acoustical Society of America*, Vol. 74, No. 6, 1983, pp. 1869–1879.

[6]Buchal, R. N., and Keller, J. B., "Boundary Layer Problems in Diffraction Theory," *Communications in Pure and Applied Mathematics*, Vol. 13, No. 1, 1960, pp. 85–114.

[7]Abrahams, I. D., Kriegsmann, G. A., and Reiss, E. L., "On the Development of Caustics in Shear Flows over Rigid Walls," *Society for Industrial and Applied Mathematics Journal of Applied Mathematics*, Vol. 49, No. 6, 1989, pp. 1652–1664.

[8]Jones, D. S., "The Scattering of Sound by a Simple Shear Layer," *Philosophical Transactions of the Royal Society of London*, Series A: Mathematical and Physical Sciences, Vol. 284, No. 1323, 1977, pp. 287–328.

[9]Abrahams, I. D., Kriegsmann, G. A., and Reiss, E. L., "On the Development and Control of Caustics in Shear Flows over Elastic Surfaces," *Journal of the Acoustical Society of America*, Vol. 92, No. 1, 1992, pp. 428–434.

[10]Smith, C. R., Walker, J. D. A., Haidari, A. H., and Sobrun, U., "On the Dynamics of Near-Wall Turbulence," *Philosophical Transactions of the Royal Society of London*, Series A: Mathematical and Physical Sciences, Vol. 336, No. 1641, 1991, pp. 131–175.

[11]Kim, J., Moin, P., and Moser, R., "Turbulence Statistics in Fully Developed Channel Flow at Low Reynolds Number," *Journal of Fluid Mechanics*, Vol. 177, April 1987, pp. 133–166.

[12]Olver, F. W. J., *Asymptotics and Special Functions*, Academic Press, New York, 1977.

[13]Cantwell, B. T., Coles, D., and Dimotakis, P., "Structure and Entrainment in the Plane of Symmetry of a Turbulent Spot," *Journal of Fluid Mechanics*, Vol. 87, No. 4, 1978, pp. 641–672.

[14]Smith, C. R., and Metzler, S. P., "The Characteristics of Low-Speed Streaks in the Near-Wall Region of a Turbulent Boundary Layer," *Journal of Fluid Mechanics*, Vol. 129, April 1983, pp. 27–54.